Article

Journal of the Brazilian Chemical Society

https://dx.doi.org/10.21577/0103-5053.20240010

J. Braz. Chem. Soc., **2024**, *35*, 7, e-20240010, 1-10

^{1}H NMR Chemical Profile and Antioxidant Activity of *Eugenia punicifolia* Extracts Over Seasons: A Metabolomic Pilot Study

Kidney O. G. Neves,[a] Maria F. C. Santos,[b] Josiana M. Mar,[c] Flávia L. D. Pontes,[d] Claudio F. Tormena,[b] Francisco C. M. Chaves,[e] Francinete R. Campos,[d] Edgar Aparecido Sanches,[c] Jaqueline A. Bezerra,[f] Marcos B. Machado *,[a] ***and Alan D. C. Santos*** *,[a]

[a]*Núcleo de Estudos Químicos de Micromoléculas da Amazônia (NEQUIMA), Universidade Federal do Amazonas, 69067-005 Manaus-AM, Brazil*

[b]*Instituto de Química, Universidade Estadual de Campinas, 13083-862 Campinas-SP, Brazil*

[c]*Laboratório de Polímeros Nanoestruturados (NANOPOL), Departamento de Física de Materiais, Universidade Federal do Amazonas, 69067-005 Manaus-AM, Brazil*

[d]*Departamento de Farmácia, Universidade Federal do Paraná, 80210-170 Curitiba-PR, Brazil*

[e]*Empresa Brasileira de Pesquisa Agropecuária - Embrapa Amazônia Ocidental, 69010-970 Manaus-AM, Brazil*

[f]*Centro Analítico, Instituto Federal de Educação, Ciência e Tecnologia do Amazonas, 69020-120 Manaus-AM, Brazil*

Eugenia punicifolia (Kunth) DC. is a medicinal plant used to treat diseases related to oxidative processes. In this work, ^{1}H nuclear magnetic resonance (NMR) spectroscopy and multivariate analysis have been employed to track the chemical changes and antioxidant activity of dimethyl sulfoxide (DMSO) extracts from *E. punicifolia* leaves over seasons. Principal component analysis (PCA) applied to ^{1}H NMR allowed discriminating DMSO extracts from leaves collected in the dry and rainy seasons and pointed out sucrose, catechin, and epicatechin as responsible for separating dry season samples and quercetin, acid gallic, glucose, and fatty acids contributed for rainy samples grouping. Notably, antioxidant assays revealed that dry season extracts exhibited a higher radical scavenging capacity. When those compounds were submitted to partial least squares-discriminant analysis (PLS-DA) only sucrose and fatty acids presented variable importance projection (VIP) score > 1, both metabolites are related somehow to the defense mechanisms of the plant. This pilot study may suggest new experimental approaches for more effectively monitoring the spectrum-effect relationship of *E. punicifolia* leaf extracts.

Keywords: Myrtaceae, medicinal plant, seasonality, PLS-DA, DPPH, ABTS

Introduction

The investigation of medicinal plants through chemical profiling has emerged as an effective approach, leading to the identification of several bioactive compounds with the potential for developing new drugs. However, the chemical profile is susceptible to environmental influences, and among these factors, seasonality stands out as a primary determinant affecting both metabolite identities within plants and their respective concentrations.[1,2]

The therapeutic effect of medicinal plants is closely linked with a specific set of metabolites, and once the contents of these active principles fluctuate, so does the therapeutic effect.[3] Hence, the timing of plant harvest is of paramount importance when considering medical uses, since the abundance of active compounds can vary significantly throughout the year. This phenomenon is well-documented in the literature. For

*e-mail: alandiegormn@gmail.com.br; marcosmachado@ufam.edu.br
Editor handled this article: Ivo M. Raimundo Jr. (Associate)
This manuscript is part of a series of publications in the Journal of the Brazilian Chemical Society by young researchers who work in Brazil or have a solid scientific connection with our country. The JBCS welcomes these young investigators who brighten the future of chemical sciences.

instance, *Calamintha nepeta* and *Phillyrea angustifolia* demonstrated heightened activity and increased levels of active compounds in colder months.[4,5] Conversely, plants like *Croton heliotropiifolius*, *Salvia fruticose*, and *Rosmarinus officinalis* exhibited higher contents of active compounds during summer and spring months.[6-8] In certain species, seasonal variations appear negligible, as evidenced by consistent alkaloid contents in *Duguetia furfuracea*.[9] Therefore, understanding the patterns of metabolite accumulation is crucial for the standardization of cultivation practices, especially in large-scale production or sustainable plant exploitation.

In the Amazon region, leaves of *Eugenia punicifolia* (Kunth) DC., a Myrtaceae species, are widely commercialized as a phytotherapeutic for the treatment of *Diabetes mellitus*.[10,11] Furthermore, studies on *E. punicifolia* leaves have associated the anti-inflammatory, antinociceptive, and gastroprotective potential with the presence of gallic acid, proanthocyanidins, gallotannin, quercetin, myricitrin, and rutin.[12] Fruits of *E. punicifolia* have also been chemically evaluated being reported the presence of sucrose, α and β-glucose, gallic acid, ellagic acid, quercetin 3-*O*-rhamnoside, kaempferol 7-*O*-rhamnoside, as well as antiglycating and antioxidant properties.[10] As *E. punicifolia* is already consumed by the local population and has market potential, investigating seasonality effects on the chemical composition becomes important and can add economic value to this species.

However, monitoring multiple compounds in very complex matrices like natural products is not a simple task. The high diversity and complexity of chemical structures and the expressive differences in metabolite concentrations make it difficult to track relevant chemical information. Despite this, analytical tools, such as nuclear magnetic resonance (NMR) and high-performance liquid chromatography hyphenated with a diode array detector and mass spectrometer (HPLC-DAD-HRMS), along with multivariate and univariate analysis methods have been successfully applied in this context; and progress has been observed on the identification and quantification of primary and secondary metabolites that are modulated by seasonal changes. Several papers dealing with that matter can be seen in the literature.[2,13-15]

Therefore, this study aims to identify the main compounds present in dimethyl sulfoxide (DMSO) extracts of *E. punicifolia* leaves using NMR and HPLC-DAD-HRMS, as well as to use ^{1}H NMR spectroscopy combined with chemometrics analysis to evaluate the influence of seasonality on their chemical composition and antioxidant potential. The results might indicate the most promising time for leaf harvesting, which is essential to explore *E. punicifolia* as herbal medicine and for the development of bioproducts.

Experimental

Materials

Deuterated dimethyl sulfoxide used in extractions and NMR analyzes was purchased from Cambridge Isotope Laboratories Inc. (Andover, Massachusetts, USA). The methanol and formic acid used in the HPLC-DAD-HRMS analyzes were purchased from Sigma-Aldrich (St. Louis, MO, USA). The reagents 6-hydroxy-2,5,7,8-tetramethylchroman-2-carboxylic acid (Trolox), 2,2-diphenyl-1-picrylhydrazyl (DPPH$^{\bullet}$), 2,2'-azino-bis(3-ethylbenzothiazoline-6-sulfonic acid) diammonium salt (ABTS$^{\bullet+}$) and methanol used in the antioxidant assays were obtained from Sigma-Aldrich (St. Louis, MO, USA).

Plant material

Leaves of *Eugenia punicifolia* species were collected at 9 am in different months (August 2021 (dry season), December 2021 (transition period), and March 2022 (rainy season)) at the Brazilian Agricultural Research Corporation-Embrapa Western Amazon, located on AM-010 Highway, km 29 (2°53'23"S 59°58'26"W). Climatic characteristics can be expressed in terms of average temperature, precipitation, solar radiation, and relative humidity reaching values of 27.4 and 26.2 ºC, 4.6 and 11.7 mm, 15,265.4 and 11,930.9 kJ m^{2}, and 72.3 and 81.7% to dry and rainy seasons, respectively, data acquired from the National Institute of Meteorology (INMET).[16] From the plantation composed of 150 individuals, 15 were randomly selected, and their leaves were collected from different parts of the tree to obtain the best representativeness *per* sample (11 leaves from the lower part, 11 from the intermediate part, and 11 from the upper part). The plant material was dried at room temperature for 24 and 48 h in a forced air circulation oven at 40 °C. After drying, each sample was subjected to the cold maceration process with liquid nitrogen, weighed, and stored in a freezer at −80 °C until the extraction procedure.

Chemical profile of the DMSO extract of *E. punicifolia* by HPLC-DAD-HRMS

For the analysis of HPLC-DAD-HRMS, 50 mg of dried leaves from a mix of the samples from the first collection were extracted with 650 µL of deuterated dimethyl sulfoxide in an ultrasonic bath for 20 min. After this time, the sample was centrifuged at 10.000 rpm

for 10 min, the supernatant (550 μL) was removed, lyophilized, and subjected to analysis. Analyses was performed on a high-performance liquid chromatograph (HPLC) (Shimadzu, Tokyo, Japan), with an autosampler maintained at 10 °C, coupled to the quadrupole time of flight high resolution mass spectrometer (Q-TOF-MS) (Bruker Daltonics, Fremont, CA, USA). A reversed-phase Synergi Fusion-RP C18 Phenomenex® column (150 × 2.1 mm, 4 μm particle size) was used with a guard column of the same phase. The mobile phase consisted of water (A) and methanol (B), both containing 0.1% formic acid. Elution was performed in gradient mode, with 0-28 min (20-100% B), 28-38 min (100% B), 38-48 min (100-20% B), 48-55 min (20% B). The flow rate was maintained at 200 μL min^{-1} and the column temperature at 40 °C. The injection volume was 2.0 μL. The parameters of the ionization source (electrospray in positive mode) were as follows: capillary potential of 4.5 kV, end plate offset of 0.5 kV, nebulizer gas pressure (nitrogen) of 2.0 bar, drying gas flow (nitrogen) of 6 L min^{-1}, and gas temperature of 180 °C. The acquisition range was from *m/z* 100 to 1000. The instrument was calibrated with 10 mM sodium formate. Data acquisition was performed with Data Analysis 4.1 software.[17]

Acquisition of NMR spectroscopy data

Fifty milligrams of *E. punicifolia* leaves were extracted with 650 μL of deuterated DMSO in an ultrasonic bath for 20 min. The sample was then centrifuged at 10.000 rpm for 10 min, the supernatant was removed, and transferred to a 5 mm NMR tube. NMR spectra were acquired on a Bruker Avance III NMR spectrometer (Bruker, Billerica, Massachusetts, USA), operating at 9.4 T, equipped with a 5 mm BBI probe with a gradient along the z-axis. NMR spectra were obtained at 25 °C using the *zgpr* pulse sequence with a 90º pulse duration of 8.58 μs. 4 dummy scans, and 64 scans were collected with 64 k data points using a spectral width of 8 kHz, a relaxation time of 1.0 s, and an acquisition time of 4.0 s. The residual water signal of DMSO-d_6 (δ_H 3.36, s) was suppressed using a power of 4.98 10^{-5} W, and the receiver gain was set to 203. Phase and baseline corrections of the spectra were performed manually using TopSpin 3.6.3 software.[18] The chemical shift (in ppm) of ^{1}H NMR spectra was referenced to the methyl signal of tetramethylsilane at δ_H 0.0. The ^{1}H-^{13}C correlations from edited heteronuclear quantum coherence (HSQCedit) and heteronuclear multiple bond correlation (HMBC) NMR experiments were acquired using the coupling constants *J* (H,C, one-bond) and *J* (H,C, long-range) of 145 and 8 Hz, respectively.

Multivariate data analysis

^{1}H NMR spectra of the 45 samples were acquired in triplicate, exported from TopSpin 3.6.3 software in .csv format and transferred to OriginPro 2018 software to build the data matrix.[18,19] Chemometric analysis was carried out using the region of ^{1}H NMR spectra between 0.55 to 7.40 ppm resulting in a matrix (135 samples × 5310 variables). The areas of residual water signal (3.30 to 3.40 ppm) and deuterated dimethyl sulfoxide (2.46 to 2.54 ppm) were excluded.

Principal component analysis (PCA) was performed using the PLS-Toolbox Solo 9.0 software.[20] Spectra preprocessing consisted of baseline correction (Automatic Weighted Least Squares, order = 2), variable alignment (Correlation Optimized Warping: Slack 5, Segment Length 50, and Alignment function Linear of the 1st Order). The data was normalized to the area and mean centered. The scores and loadings graphs were plotted using the algorithm Singular Value Decomposition (SVD).

Data processing and construction of the PLS-DA calibration model

To perform partial least squares-discriminant analysis (PLS-DA), the ^{1}H NMR spectra of the 135 *E. punicifolia* samples were exported to R-Studio software version 2022.07.2.[21] Subsequently, the spectral region from 0.05 to 8.20 ppm was aligned, and the residual water signal region of DMSO-d_6 was excluded. The spectra were then divided into 0.04 ppm buckets with a 50% degree of freedom, resulting in a table of 135 samples and 245 variables. This table was exported to The Unscrambler 10.3 software, where it was normalized based on total intensity (each bucket's intensity was divided by the sum of all bucket intensities in the spectrum), resulting in optimal data optimization for metabolomics studies, as described by Wang *et al.*[22,23]

The intensities of the buckets corresponding to the signals of sucrose (δ_H 5.18, *d*, 3.7 Hz), catechin (δ_H 5.93, d, 2.3 Hz), epicatechin (δ_H 5.89, d, 2.2 Hz), fatty acids (δ_H 1.23, s), α-glucose (δ_H 4.90, d, 3.6 Hz), β-glucose (δ_H 4.27, d, 7.8 Hz), gallic acid (δ_H 6.95, s), and quercetin (δ_H 7.30, d, 2.3 Hz) were exported from The Unscrambler 10.3 software and transferred to MetaboAnalyst 5.0, where they were scaled using the autoscaling method (mean-centered and divided by the standard deviation of each variable).[24,25] After scaling, the data were used to build the PLS-DA calibration model, which underwent cross-validation (method 5-fold CV), permutation testing

(separation distance adjusted to 2000 permutation), and the construction of Vip score plots.

DPPH radical scavenging capacity

The experiments were carried out following the methods described in a previous study.[26] The radical scavenging capacity of *E. punicifolia* sample after various treatment processes was assessed using the DPPH$^{\bullet}$ radical method. A 100 μM methanolic DPPH$^{\bullet}$ solution was prepared. Then, the sample was prepared at a concentration of 1 mg mL^{-1} and mixed with 1900 μL of the methanolic DPPH$^{\bullet}$ radical solution. Trolox was used as a positive control (ranging from 100 to 2000 μM) for comparison. The mixture was incubated in darkness at room temperature for 30 min. Absorbance readings were taken at 515 nm using a microplate reader (Bio Tek Instruments Inc., Winooski, VT, USA). The antioxidant capacity was quantified in Trolox equivalents. The assay was performed in triplicate. The relationship was determined as $y = -0.0004x + 0.7126$, with coefficient of determination (R^2) value of 0.9926, and the results were expressed in micromolar Trolox Equivalents (μM TE mL^{-1}).

ABTS radical cation scavenging capacity

The ABTS$^{\bullet+}$ scavenging assay entails observing the fading of the ABTS$^{\bullet+}$ solution color in the presence of antioxidant extracts.[26,27] Following a reaction period of 6 min between the sample and the radical at a 1:10 ratio, absorbances were recorded at 750 nm using a microplate reader (Bio Tek Instruments Inc., Winooski, VT, USA). Trolox was employed to construct the standard curve ($y = 0.0003x + 0.7216$, $R^2 = 0.9951$), and the results were quantified in micromolar Trolox Equivalents (μM Trolox mL^{-1}).

Statistical analysis

The distribution of antioxidant data for DPPH radical and ABTS radical cation, as well as to the area of the signs of sucrose (δ_H 5.18, d) and fatty acids (δ_H 1.23, s) were assessed using the normality test (Kolmogorov-Smirnov), followed by the Kruskal-Wallis nonparametric test for data with a non-normal distribution. The comparison among multiple data sets with a normal distribution was performed using ANOVA (variance analysis) with the Tukey's test, at a significance level of 95%. Pearson correlation coefficients were obtained with a p-value of < 0.05. The analyses were conducted using Minitab™ 18.1 software.[28]

Results and Discussion

Chemical profiles of *E. punicifolia* extracts via HPLC-DAD-HRMS and NMR spectroscopy

HPLC-DAD-HRMS profiles of DMSO-d_6 extracts from *E. punicifolia* revealed the presence of 10 flavonoids (Table 1). The identification of these compounds was achieved through an analysis of their ion fragmentation patterns (Figures S1-S18, Supplementary Information (SI) section), as well as by comparison with mass spectrometry (MS) data previously documented in the literature for *Eugenia* species. DMSO extracts were submitted to NMR spectroscopy, and spectra of hydrogen revealed a typical complex profile with signals in the aliphatic, carbinolic, and aromatic regions (Figures S19-S21, SI section). To endorse the compound identities in ^{1}H NMR spectra, 2D NMR experiments, such as (^{1}H-^{1}H) correlated spectroscopy (COSY), (^{1}H-^{13}C) HSQCedit, and (^{1}H-^{13}C) HMBC, were also obtained (Figures S22-S30, SI section).

Characteristic signals of fatty acids (**1**) and carbohydrates (**2-4**) were observed, as previously reported.[10] Also, three flavonoids were identified: catechin (**5**), epicatechin (**6**), and quercetin (**7**). For catechin, the signals at δ_H 5.83 (d, 2.3 Hz), δ_H 5.93 (d, 2.3 Hz), δ_H 6.86 (d, 2.3 Hz), δ_H 6.66 (d, 8.1 Hz) and δ_H 6.75 (dd, 2.3 and 8.1 Hz), related to position 6, 8, 2', 5' and 6' of rings A and B were assigned.[29] The epicatechin A-ring showed resonances at δ_H 5.89 (d, 2.2 Hz) and δ_H 5.88 (d, 2.2 Hz).[30] While for quercetin, the signals attributed were δ_H 7.30 (d, 2.1 Hz), δ_H 7.25 (dd, 2.1 Hz and 8.4 Hz), and δ_H 6.87 (d, 8.4 Hz), related to quercetin C-ring, as well as signals at δ 6.40 (d, 2.1 Hz) and δ_H 6.21 (d, 2.1 Hz), characteristic of ring A of quercetin.[28] Finally, signals at δ_H 6.95 (s) and δ_H 6.82 (s) showed correlations to δ_C 165.9, δ_C 108.6, δ_C145.7, and δ_C 138.3 in the HMBC experiment indicating the presence of gallic acid (**8**) and derivatives.[31] Figure 1 depicts the compounds identified.

Multivariate NMR data analysis

^{1}H NMR spectra of *E. punicifolia* were submitted to PCA analysis aiming to discriminate the sample groups by season and to track the compounds responsible for such grouping. Scores and loadings plots are depicted in Figures 2 and 3. The two first principal components explained 65.82% of the total variance. Samples from drought and rainy periods occupied the positive and negative sides of PC1, respectively. Samples collected in the transition season could be found spread all over the

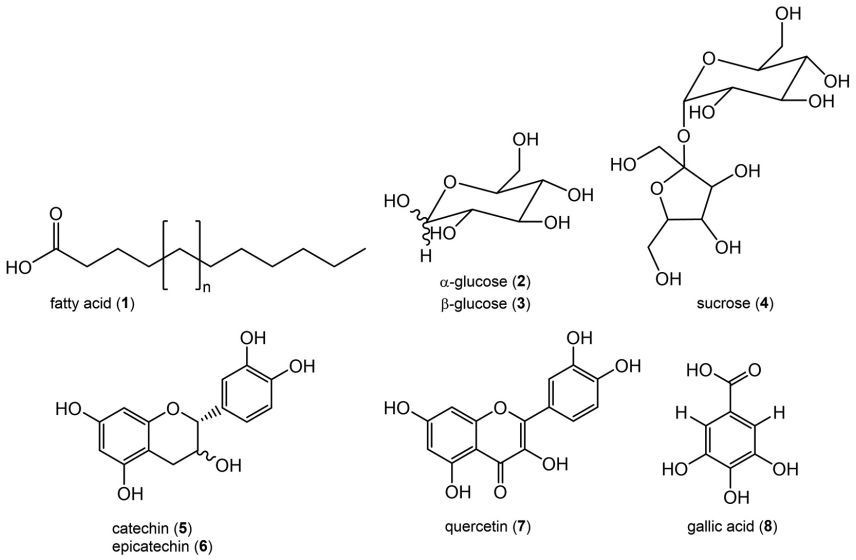

Figure 1. Compounds identified by NMR spectroscopy analysis of DMSO-d_6 extracts from *E. punicifolia*.

Table 1. Compounds identified in DMSO extract from *E. punicifolia* leaves by HPLC-DAD-HRMS

t_r / min	Compound	Molecular formula	Meas.[a] (*m*/*z*)	Calcd.[b] (*m*/*z*)	Error / ppm	MS/MS[c]	Reference
5.0	epicatechin	$C_{15}H_{14}O_6^+$	291.086571	291.086315	0.88	139	32,33
5.2	epigallocatechin gallate	$C_{22}H_{18}O_{11}^+$	459.090472	459.092188	–3.74	289, 139	34,35
7.0	catechin gallate	$C_{22}H_{18}O_{10}^+$	443.097327	443.097273	0.12	291, 273, 139	33,36
8.7	epicatechin 3-*O*-(3-*O*-methylgallate)	$C_{23}H_{20}O_{10}^+$	457.112003	457.112923	–2.01	273, 167, 151, 139	37,38
10.2	Myricitrin myricetin	$C_{21}H_{20}O_{12}^+$ $C_{15}H_{10}O_8^+$	465.102519 319.045936	465.102753 319.044844	–0.50 3.42	319, 303, 153 153	29,39 40,41
12.1	Quercitrin quercetin	$C_{21}H_{20}O_{11}^+$ $C_{15}H_{10}O_7^+$	449.108278 303.050967	449.107838 303.049929	0.98 3.43	303 229, 153	34,42 36,43
13.7	kaempferol-7-rhamnoside kaempferol	$C_{21}H_{20}O_{10}^+$ $C_{15}H_{10}O_6^+$	433.112825 287.055621	433,112923 287.055014	–0.23 2.11	287 153	10,44 45,46

[a]Measured; [b]calculated; [c]main fragments.

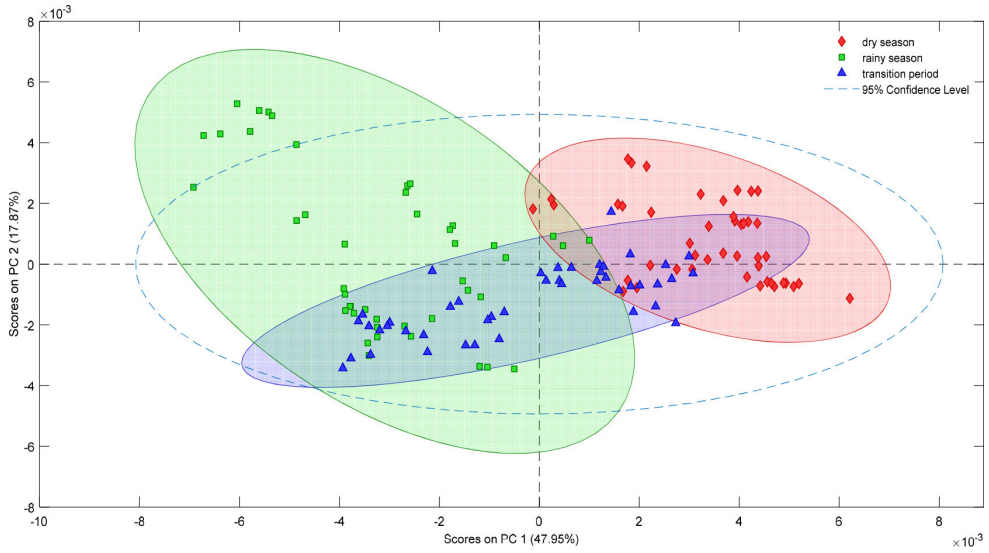

Figure 2. Principal components analysis (PCA) of DMSO extracts of *E. punicifolia*. Scores plot of PC1 (47.95%) *versus* PC2 (17.87%). Samples falling outside the 95% confidence level were not designated as outliers, as there were no identified issues with sample collection, extraction procedures, or data acquisition and processing. These samples exhibited lower sucrose contents compared to the remaining samples collected during the dry season.

scores plot, some of them having chemical profiles like rainy samples and others more like drought samples.

According to the loadings plot (Figure 3), sucrose (δ_H 5.18, d, 3.7 Hz), catechin (δ_H 5.93, d, 2.3 Hz) and epicatechin (δ_H 5.89, d, 2.2 Hz) influenced the discrimination of drought period samples, while fatty acids (δ_H 1.23, s), α-glucose (δ_H 4.90, d, 3.6 Hz), β-glucose (δ_H 4.27, d, 7.8 Hz), gallic acid (δ_H 6.95, s), and quercetin (δ_H 7.30, d, 2.3 Hz) were responsible for the grouping of samples of rainy period in the negative region of PC1. Of note, the transition samples mostly occupied the negative side of PC2, yet shared similar chemical characteristics with certain rainy and drought samples. Upon examining the loadings plot of PC2, it was possible to identify the α-glucose (δ_H 4.90, d, 3.6 Hz) as responsible for samples in the negative side of PC2, while β-glucose, gallic acid, sucrose, and predominantly fatty acids were identified in positive PC2 (Figure S32, SI section).

PLS-DA calibration model

The PLS-DA model was constructed using normalized and autoscaled intensities of buckets from the compounds indicated by PCA analysis: sucrose (δ_H 5.18, d, 3.7 Hz), catechin (δ_H 5.93, d, 2.3 Hz), epicatechin (δ_H 5.89, d, 2.2 Hz), fatty acids (δ_H 1.23, s), α-glucose (δ_H 4.90, d, 3.6 Hz), β-glucose (δ_H 4.27, d, 7.8 Hz), gallic acid (δ_H 6.95, s), and quercetin (δ_H 7.30, d, 2.3 Hz). PLS-DA has been used as a discriminative variable selection, allowing tracking of the contribution of each input information to the prediction model.[47,48] Once samples from the transition period had chemical features similar to samples from dry and rainy seasons, we kept them out in this part of the study.

Component 1 (57.3%) of the PLS-DA model was responsible for separating samples collected during the dry and rainy periods, as illustrated in Figure 4a. Estimation of the model's quality was performed using the cross-validation method through values of accuracy, Q^2, and R^2.[49-51] Q^2 indicates the predictive capability of the model, while R^2 represents the model's ability to explain the data and predict new observations.[50,51] Based on Table 2, one can be observed that Q^2 and R^2 have similar magnitudes for all calculated components, indicating the absence of overfitting, and accuracy values above 90%. To demonstrate that the values obtained from the cross-validation method were not acquired by chance, a permutation test was conducted. In this test, *p*-values < 0.05 suggest that the obtained data is significant. Q^2 was chosen as the statistical parameter for the permutation test, resulting in a *p*-value < 0.0005, which confirms the validity of the model.

After validating the model, the variable importance projection (VIP) scores were used to judge the importance of a compound (bucket area) in explaining the chemical variation over the seasons (Figure 4b). Normally, variables with VIP score greater than 1 are considered relevant to the model with an important contribution to explaining the dependent variable.[52] It becomes evident that sucrose and fatty acids emerge as responsible for discriminating samples from the dry and rainy periods, respectively. Conversely, the remaining compounds exhibited VIP scores below 1.

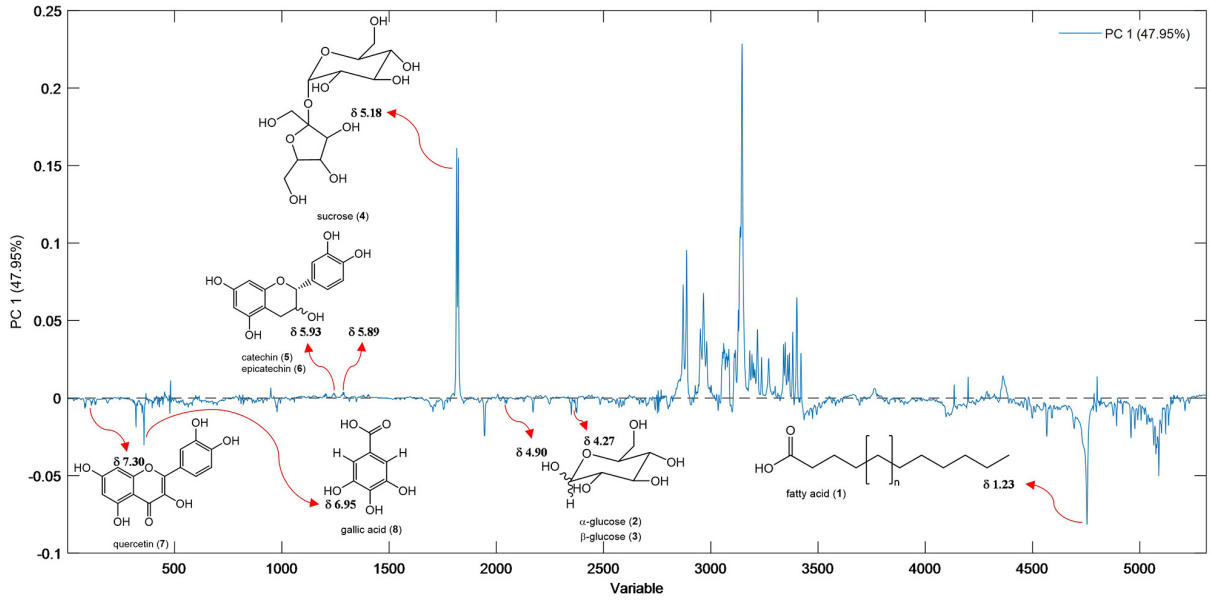

Figure 3. Loadings plot of PC1 discriminating the compounds responsible for the grouping of samples of *E. punicifolia*. Data obtained by [1]H NMR (400 MHz, DMSO-d_6).

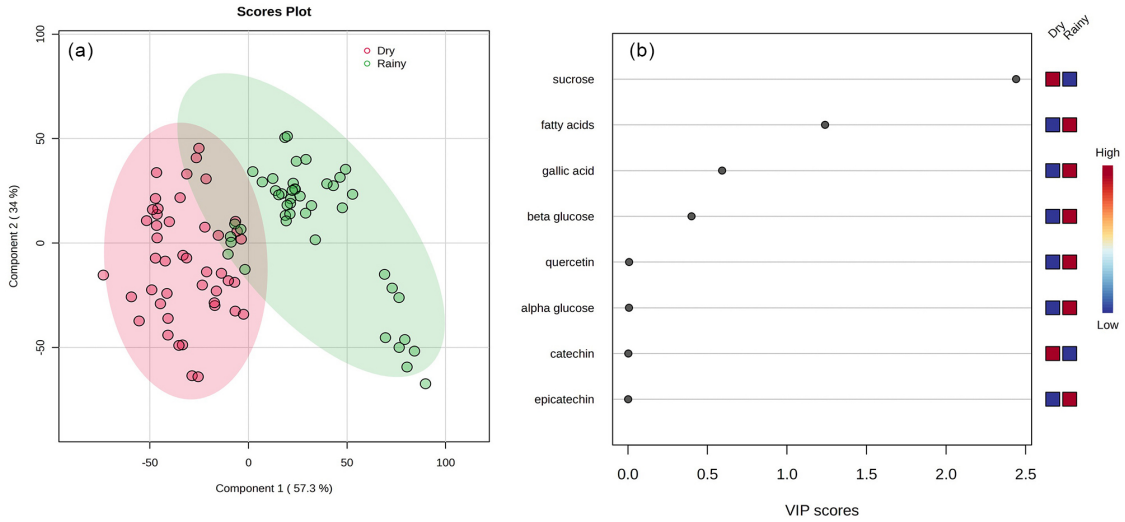

Figure 4. PLS-DA score plot showing the separation of dry and rainy samples (a), and graph of VIP scores (b).

Table 2. Accuracy, R^2, and Q^2 values obtained in the cross-validation of the PLS-DA model as a function of the number of components (comps) used

Measure	1 comps	2 comps	3 comps	4 comps	5 comps
Accuracy	0.9333	0.9333	0.9333	0.9333	0.9444
R^2	0.6613	0.7469	0.8011	0.8049	0.8414
Q^2	0.6481	0.7342	0.7831	0.7853	0.7966

Q^2: predictive capability of the model; R^2: model's ability to explain the data and predict new observations.

Table 3. Scavenging capacity of the free radical DPPH$^{\bullet}$ and the cation radical ABTS$^{\bullet+}$

Season	DPPH$^{\bullet}$ SC ± SD / (μM TE g^{-1})	ABTS$^{\bullet+}$ SC ± SD / (μM TE g^{-1})
Dry	1208.0 ± 112.6^{a}	1641.2 ± 147.5^{a}
Transition	1160.7 ± 108.8^{ab}	1567.6 ± 145.6^{b}
Rainy	1132.1 ± 114.6^{b}	1465.3 ± 120.6^{c}

^{a,b,c}Clustering for DPPH$^{\bullet}$ and ABTS$^{\bullet+}$ assay using Tukey's method and 95% confidence interval; SC: scavenging capability expressed in micromolar Trolox Equivalents (μM TE mL^{-1}); SD: standard deviation; DPPH•: 2,2-diphenyl-1-picrylhydrazyl; ABTS•+: 2,2'-azino-bis(3-ethylbenzothiazoline-6-sulfonic acid) diammonium salt.

Antioxidant potential of DMSO extracts from leaves of *E. punicifolia*

DMSO extracts from *E. punicifolia* leaves were submitted to assays for scavenging the free radical DPPH and the cation radical ABTS. Fifteen samples from each period were employed in those experiments. The analysis of DPPH$^{\bullet}$ data variance resulted in the formation of two groups: group A, composed of samples from dry and transition periods, and group B, comprising samples from transition and rainy periods. While for the ABTS$^{\bullet+}$ assay, three groups were observed, corresponding to each collection period (Table 3). Notably, despite the slight differences between the assays, samples obtained during the dry period exhibited a superior scavenging capacity in both assays. The Pearson correlation between the DPPH$^{\bullet}$ and ABTS$^{\bullet+}$ assays was 0.85 ($p < 0.05$) which indicates a moderate and positive correlation and strengthens the presence of antioxidant properties of DMSO extracts from *E. punicifolia* leaves.

[1]H NMR chemical profiles and antioxidant activities of DMSO extracts

The environmental stress, provoked by the water scarcity and higher indexes of solar radiation and temperatures, inherent to the dry seasons, intensifies the oxidative stress in plants, which in turn, triggers their defense mechanisms to minimize oxidative damage to cells.

As reviewed by Liebelt *et al.*,[53] seasonal effects on antioxidants are diverse. Small water-soluble sugars, such as sucrose, have been recognized as crucial in orchestrating plant developmental responses under oxidative stress, not only as a consequence of remodeling carbon metabolism or signaling, but acting as an antioxidant itself, or serving as a substrate to the synthesis of oligosaccharides also with antioxidant properties.[54,55] According to Uemura and Steponkus,[56] at low concentrations, sucrose might serve as a substrate or signal for stress-induced alterations, while, at high concentrations, it can directly play a protective agent role. That might explain the increase in sucrose content and antioxidant activity in the DMSO extracts of *E. punicifolia* leaves obtained in the dry season.

Furthermore, literature underscores sucrose's role in the accumulation of phenolic compounds and the improvement of antioxidant activity.[57-59] Unfortunately, the chemical

profiles acquired in our work did not allow us to visualize such a trend. To overcome that, a target extraction method should be investigated which can lead to the acquisition of phenolic-rich NMR profiles enabling the correlation between secondary metabolites and antioxidant activity. A closer look at MS data indicates a richer phenolic composition than that registered by NMR data, and those compounds, even in lower concentrations, can contribute significantly to the bioactivity observed. That is quite reasonable once the antioxidant activity of a compound depends on its chemical structure, for example, phenolic compounds glycosylated have shown stronger activity than not glycosylated ones.[55]

Conversely, during the rainy season, there was an increase in the normalized area of fatty acids suggesting an alteration in the lipid metabolism. At high average relative humidity and rainfall rates, plants become more susceptible to pathogen attacks, like fungi.[60] Oxylipins and unsaturated fatty acids play an important role in signaling functions during plant-pathogen interaction. Besides that, the very long chain fatty acid (VLCFA) biosynthesis pathway has been associated with plant defense through different aspects, including the biosynthesis of sphingolipids, which is a signaling component, and the production of the plant cuticle, which can change its composition because of the pathogen attack. Of note, one of the ways plants synthesize VLCFA is through the elongation of the C16 and C18 fatty acids, which can explain the increase in fatty acid production.[61,62]

Conclusions

Through HPLC-DAD-HRMS and NMR spectroscopy, fifteen compounds were identified in DMSO extracts from *E. punicifolia* leaves. The chemical information obtained via ^{1}H NMR spectroscopy was enough to discriminate *E. punicifolia* leaves collected in dry and rainy seasons via PCA. Also, antioxidant assays showed extracts from the dry season with higher radical scavenging capacity. PLS-DA of the metabolites pointed out sucrose and fatty acids as mainly responsible for the grouping of samples. These results suggest that the dry season had an impact on carbon metabolism as a consequence of the oxidative stress and the triggering of antioxidant mechanisms. Similarly, the rainy season appeared to influence lipid metabolism, which is related to plant protection against pathogen attacks. This preliminary investigation will provide a foundation for our forthcoming study, wherein we will examine month-to-month fluctuation in chemical profiles acquired through a phenolic-driven extraction method. Our aim is to enhance the methodology capacity to uncover correlations between secondary metabolites and bioactivity. Knowledge of this spectrum-effect relationship aggregates value to *E. punicifolia* and might suggest the most appropriate season for developing *E. punicifolia* leaves-based bioproducts and exploring it as herbal medicine.

Supplementary Information

Supplementary data (HRMS spectra and NMR spectra) are available free of charge at http://jbcs.sbq.org.br as PDF file.

Acknowledgments

The authors would like to thank Fundação de Amparo à Pesquisa do Estado do Amazonas-FAPEAM (EDITAL No. 013/2022-PRODUTIVIDADE-CT&I), Resolução No. 002/2023-PROSGRAD 2023/2024-Coordenador/Auxílio Financeiro/PPGQ) the Postgraduate Program in Chemistry at the Federal University of Amazonas (PPGQ-UFAM), and Nuclear Magnetic Resonance Laboratory (NMRLab) of the Analytical Center of UFAM for the financial support, fellowships, and infrastructure, and Dr Otávio Neto for curating climate date.

Author Contributions

Kidney O. G. Neves, Marcos B. Machado, and Alan D. C. Santos contributed to the conceptualization of the project and manuscript writing; Josiana M. Mar, Edgar A. Sanches, and Jaqueline A. Bezerra provided the materials and reagents necessary for conducting the antioxidant assays, as well as performing the assays themselves; Flávia L. D. Pontes and Francinete R. Campos were responsible for acquiring the HPLC-DAD-HRMS spectra; Francisco C. M. Chaves was in charge of identifying and collecting botanical material, as well as obtaining meteorological data; Maria F. C. Santos and Claudio F. Tormena facilitated the acquisition and interpretation of NMR data.

References

1. Aru, V.; Engelsen, S. B.; Savorani, F.; Culurgioni, J.; Sarais, G.; Atzori, G.; Cabiddu, S.; Marincola, F. C.; *Metabolites* **2017**, *7*, 36. [Crossref]
2. Aves Filho, E. G.; Silva, L. M. A.; Ribeiro, P. R. V.; de Brito, E. S.; Zocolo, G. J.; Souza-Leão, P. C.; Marques, A. T. B.; Quintela, A. L.; Larsen, F. H.; Canuto, K.; *Food Chem.* **2019**, *289*, 558. [Crossref]
3. Zanatta, A. C.; Vilegas, W.; Edrada-Ebel, R.; *Front. Chem.* **2021**, *9*, 710025. [Crossref]
4. Pacifico, S.; Galasso, S.; Piccolella, S.; Kretschmer, N.; Pan, S.-P.; Marciano, S.; Bauer, R.; Monaco, P.; *Food Res. Int.* **2015**, *69*, 121. [Crossref]

5. Scognamiglio, M.; D'Abrosca, B.; Fiumano, V.; Golino, M.; Esposito, A.; Fiorentino, A.; *Phytochem Lett.* **2014**, *8*, 163. [Crossref]
6. de Alencar Filho, J. M. T.; Araújo, L. C.; Oliveira, A. P.; Guimarães, A. L.; Pacheco, A. G. M.; Silva, F. S.; Cavalcanti, L. S.; Lucchese, A. M.; Almeida, J. R. G. S.; Araújo, E. C. C.; *Rev. Bras. Farmacogn.* **2017**, *27*, 440. [Crossref]
7. Sarrou, E.; Martens, S.; Chatzopoulou, P.; *Ind. Crops Prod.* **2016**, *94*, 240. [Crossref]
8. Lemos, M. F.; Lemos, M. F.; Pacheco, H. P.; Endringer, D. C.; Scherer, R.; *Ind. Crops Prod.* **2015**, *70*, 41. [Crossref]
9. Macedo, A. L.; Boaretto, A. G.; da Silva, A. N.; Maia, D. S.; de Siqueira, J. M.; Silva, D. B.; Carollo, C. A.; *J. Braz. Chem. Soc.* **2021**, *32*, 1840. [Crossref]
10. Ramos, A. S.; Mar, J. M.; da Silva, L. S.; Acho, L. D. R.; Silva, B. J. P.; Lima, E. S.; Campelo, P. H.; Sanches, E. A.; de Araujo Bezerra, J.; Chaves, F. C. M.; Campos, F. R.; Machado, M. B.; *Food Res. Int.* **2019**, *123*, 674. [Crossref]
11. de Souza, A. M.; de Oliveira, C. F.; de Oliveira, V. D.; Betim, F. C. M.; Miguel, M. D.; *Planta Med.* **2018**, *84*, 1232. [Crossref]
12. Basting, R. T.; Nishijima, C. M.; Lopes, J. A.; Santos, R. C.; Lucena Périco, L.; Laufer, S.; Bauer, S.; Costa, M. F.; Santos, L. C.; Rocha, L. R. M.; Vilegas, W.; Santos, A. R. S.; dos Santos, C.; Hiruma-Lima, C. A.; *J. Ethnopharmacol.* **2014**, *157*, 257. [Crossref]
13. Larive, C. K.; Barding, G. A.; Dinges, M. M.; *Anal. Chem.* **2014**, *87*, 133. [Crossref]
14. Zhuang, H.; Ni, Y.; Kokot, S.; *Chemom. Intell. Lab. Syst.* **2014**, *135*, 183. [Crossref]
15. Santos, M. F. C.; Rech, K. S.; Dutra, L. M.; Menezes, L. R. A.; Santos, A. D. C.; Nagata, N.; Stefanello, M. É. A.; Barison, A.; *Food Chem.* **2023**, *408*, 135016. [Crossref]
16. National Institute of Meteorology (INMET); *Annual Meteorological Data of Brazil*; https://portal.inmet.gov.br/, accessed on September 9th, 2022.
17. *Data Analysis*, version 4.1; Bruker Daltonics; Billerica, MA, USA, 2017.
18. *TopSpin*, version 3.6.3; Academia License, Bruker Optics GmbH & Co. KG; Ettlingen, Germany, 2021.
19. *OriginPro*, version 2018; OriginLab Corporation; Northampton, MA, USA, 2018.
20. *PLS-Toolbox Solo*, version 9.0; Eigenvector Research Inc.; Wenatchee, WA, USA, 2021.
21. *RStudio: Integrated Development Environment for R*; RStudio, PBC; Boston, MA, USA, 2020.
22. Wang, B.; Goodpaster, A.; Kennedy, M. A.; *Chemom. Intell. Lab. Syst.* **2013**, *128*, 9. [Crossref]
23. *The Unscrambler*, version 10.3; CAMO software AS; Oslo, Norway, 2012.
24. Xia, J.; Psychogios, N.; Young, N.; Wishart, D. S.; *Nucleic Acids Res.* **2009**, *37*, W652. [Crossref]
25. Pang, Z.; Chong, J.; Zhou, G.; Morais, D. A. L.; Chang, L.; Barrette, M.; Gauthier, C.; Jacques, P.-É.; Li, S.; Xia, J.; *Nucleic Acids Res.* **2021**, *49*, W388. [Crossref]
26. Mar, J. M.; da Silva, L. S.; Moreira, W. P.; Biondo, M. M.; Pontes, F. L. D.; Campos, F. R.; Kinupp, V. F.; Campelo, P. H.; Sanches, E. A.; Bezerra, J. A.; *Food Chem.* **2021**, *356*, 129723. [Crossref]
27. Aquino Neto, F. R.; *Cromatografia: Princípios Básicos e Técnicas Afins*, vol. 1, 1st ed.; Interciência: Rio de Janeiro, Brazil, 2003.
28. *Minitab*, version 18.1; Minitab Inc.; State College, PA, USA, 2017.
29. Oliveira, E. S. C.; Acho, L. D. R.; da Silva, B. J. P.; Morales-Gamba, R. D.; Pontes, F. L. D.; do Rosário, A. S.; Bezerra, J. A.; Campos, F. R.; Barcellos, J. F. M.; Lima, E. S.; Machado, M. B.; *J. Ethnopharmacol.* **2022**, *293*, 115276. [Crossref]
30. Napolitano, J. C.; Gödecke, T.; Lankin, D. C.; Jaki, B.; McAlpine, J. B.; Chen, S.-N.; Pauli, G. F.; *J. Pharm. Biomed. Anal.* **2013**, *93*, 59. [Crossref]
31. López-Martínez, L.; Santacruz-Ortega, H.; Navarro, R.; Sotelo-Mundo, R.; González-Aguilar, G. A.; *PLoS ONE* **2015**, *10*, 0140242. [Crossref]
32. Soares, J. C.; Rosalen, P. L.; Lazarini, J. G.; Massarioli, A. P.; da Silva, C. F.; Nani, B. D.; Franchin, M.; de Alencar, S. M.; *Food Chem.* **2019**, *281*, 178. [Crossref]
33. Chang, C.-L.; Wu, R.-T.; *Food Chem.* **2011**, *126*, 710. [Crossref]
34. da Silva, G. L.; Campideli, M. B.; Ferrari, A. B. S.; Mannochio-Russo, H.; Fraige, K.; Dametto, A. C.; Bolzani, V. S.; Zeraik, M. L.; *Nat. Prod. Res.* **2021**, *36*, 4724. [Crossref]
35. Spáčil, Z.; Nováková, L.; Solich, P.; *Food Chem.* **2010**, *123*, 535. [Crossref]
36. Siebert, D. A.; Bastos, J.; Spudeit, D. A.; Micke, G. A.; Alberton, M. D.; *Ver. Bras. Farmacogn.* **2017**, *27*, 459. [Crossref]
37. Tan, J.; Dai, W.; Lu, M.; Lv, H.; Guo, L.; Zhang, Y.; Zhu, Y.; Peng, Q.; Lin, Z.; *Food Res. Int.* **2016**, *79*, 106. [Crossref]
38. Dou, J.; Lee, V. S. Y.; Tzen, J. T. C.; Lee, M.-R.; *J. Agric. Food Chem.* **2007**, *55*, 7462. [Crossref]
39. Hwang, I. W.; Chung, S. K.; *Prev. Nutr. Food Sci.* **2018**, *23*, 341. [Crossref]
40. Borges, K. C.; Bezerra, M. F.; Rocha, P. M.; Silva, E. S. D.; Fujita, A.; Genovese, M. I.; Correia, R. T. P.; *J. Prob. Health* **2016**, *4*, 100145. [Crossref]
41. Mbeunkui, F.; Grace, M. H.; Yousef, G. G.; Ann Lila, M.; *J. Sep. Sci.* **2012**, *35*, 1682. [Crossref]
42. Pacheco, A. G. M.; Branco, A.; Câmara, C. A.; Silva, T. M. S.; Silva, T. M. G.; Oliveira, A. P.; Santos, A. D. C.; Dutra, L. M.; Rolim, L. A.; Oliveira, G. G.; *Nat. Prod. Res.* **2021**, *35*, 2414. [Crossref]
43. Tsimogiannis, D.; Samiotaki, M.; Panayotou, G.; Oreopoulou, V.; *Molecules* **2007**, *12*, 593. [Crossref]

44. Sharaf, M.; El-Ansari, M. A.; Saleh, N. A. M.; *Biochem. Syst. Ecol.* **1997**, *25*, 161. [Crossref]
45. John, K. M.; Ayyanar, M.; Subbiah, J.; Murugesan, S.; Gansukh, E.; Kim, D.; *BioMed Res. Int.* **2014**, *2014*, ID726145. [Crossref]
46. Ma, C.; Lv, H.; Zhang, X.; Chen, Z.; Shi, J.; Lu, M.; Lin, Z.; *Anal. Chim. Acta* **2013**, *795*, 15. [Crossref]
47. Lee, L. C.; Liong, C. Y.; Jemain, A. A.; *Analyst* **2018**, *143*, 3526. [Crossref]
48. Zheng, R.; Chen, Z.; Guan, Z.; Zhao, C.; Cui, H.; Shang, H.; *Chin. Med.* **2023**, *18*, 15. [Crossref]
49. Cruciani, G.; Baroni, M.; Clementi, S.; Costantino, G.; Riganelli, D.; Skagerberg, B.; *J. Chemom.* **1992**, *6*, 335. [Crossref]
50. Szymańska, E.; Saccenti, E.; Smilde, A. K.; Westerhuis, J. A.; *Metabolomics* **2012**, *8*, 3. [Crossref]
51. Westerhuis, J. A.; van Velzen, E. J. J.; Hoefsloot, H. C. J.; Smilde, A. K.; *Metabolomics* **2008**, *4*, 293. [Crossref]
52. Akarachantachote, N.; Chadcham, S.; Saithanu, K.; *Int. J. Pure Apll. Math.* **2014**, *94*, 3. [Crossref]
53. Liebelt, D. J.; Jordan, J. T.; Doherty, C. J.; *Phytochem. Rev.* **2019**, *18*, 1409. [Crossref]
54. Scarpeci, T. E.; Valle, E. M.; *Plant Growth Regul.* **2008**, *54*, 133. [Crossref]
55. Van den Ende, W.; Valluru, R.; *J. Exp. Bot.* **2009**, *60*, 9. [Crossref]
56. Uemura, M.; Steponkus, P. L.; *Plant Cell Environ.* **2003**, *26*, 1083. [Crossref]
57. Nguyen, B. C. Q.; Shahinozzaman, M.; Tien, N. T. K.; Thach, T. N.; Tawata, S.; *J. Cereal Sci.* **2020**, *93*, 102985. [Crossref]
58. Jeong, H.; Sung, J.; Yang, J.; Kim, Y.; Jeong, H. S.; Lee, J.; *J. Funct. Foods* **2018**, *43*, 70. [Crossref]
59. Guo, R.; Yuan, G.; Wang, Q.; *Food Chem.* **2011**, *129*, 1080. [Crossref]
60. Gottlieb, O. R.; *Micromolecular Evolution, Systematics, and Ecology: An Essay into a Novel Botanical Discipline*; Springer-Verlag: Berlin, Germany, 1982.
61. Raffaele, S.; Leger, A.; Roby, D.; *Plant Signaling Behav.* **2009**, *4*, 94. [Crossref]
62. He, M.; Ding, N.-Z.; *Front. Plant Sci.* **2020**, *11*, 562785. [Crossref]

Submitted: October 6, 2023
Published online: January 24, 2024